Current Cardiovascular Imaging Reports (2019) 12: 7
https://doi.org/10.1007/s12410-019-9482-8

CARDIAC NUCLEAR IMAGING (A CUOCOLO AND M PETRETTA, SECTION EDITORS)

Radionuclide Imaging in Chagas Cardiomyopathy

Marcus Vinicius Simões [1,2] · Leonardo Pippa Gadioli [1] · Luciano Fonseca Lemos de Oliveira [1]

Published online: 12 February 2019

Abstract

Purpose of Review To review the contributions of radionuclide imaging to understanding the manifestations and pathophysiology of chronic Chagas cardiomyopathy (CCC).

Recent Findings Experimental studies using high-resolution SPECT myocardial perfusion imaging (MPI) show that myocardial perfusion derangement that corresponds to dysfunctional, viable myocardium is closely linked to inflammation and precedes LV regional systolic dysfunction. Clinical studies show that microvascular ischemia is strictly related to the areas of cardiac sympathetic denervation, assessed by ^{123}I-MIBG imaging, which correlates with severe ventricular arrhythmia incidence. Initial case reports suggest that ^{18}F-FDG-PET imaging is a promising, non-invasive detection method for myocardial inflammation.

Summary Available evidence indicates that microvascular ischemia participates in the mechanisms causing myocardial injury in CCC, with potential implication for monitoring subclinical disease progression. Moreover, MIBG imaging is a promising tool for risk stratification of sudden death. Preliminary clinical experience suggests a role for ^{18}F-FDG-PET in detection of inflammation in CCC.

Keywords Chagas disease · Cardiomyopathy · Radionuclide imaging · Scintigraphy · Myocardial perfusion · Myocarditis

Introduction

Chagas disease (CD) is caused by infection with a blood protozoan, *Trypanosoma cruzi* (*T. cruzi*), which is usually transmitted through the feces of a kissing bug, but its transmission routes also include congenital, blood transfusion, oral transmission, laboratory contamination, and organ transplantation [1, 2].

CD is a serious health problem in endemic Latin America countries; an estimated 6 million people are infected with *T. cruzi*, leading to significant morbidity and mortality. Due to migratory waves, *T. cruzi*-infected individuals have spread worldwide; an estimated 400,000 infected persons are now living in non-endemic countries, mainly in the USA and Europe [3, 4].

The natural evolution of the disease includes two distinct acute and chronic phases. The acute phase, which follows a variable incubation period that depends on the transmission route, is usually a benign febrile disease lasting 4 to 8 weeks. After this initial phase abates, infected patients progress to a long chronic phase in which the majority (70%) remain asymptomatic and free of structural organ lesions for their life span, despite positive serologic tests, constituting the chronic indeterminate phase [5]. Two to three decades after the initial *T. cruzi* infection, approximately 30% of the chronically infected patients develop organic disease manifested by digestive tract or cardiac involvement. The most severe clinical form is chronic Chagas cardiomyopathy (CCC) [6].

The essential pathologic feature of CCC is a low-grade chronic and relentless focal myocarditis that is initially clinically silent but causes progressive myocardial damage with extensive reparative interstitial fibrosis that ultimately leads to a severe form of dilated cardiomyopathy [7]. This global

This article is part of the Topical Collection on *Cardiac Nuclear Imaging*

✉ Marcus Vinicius Simões
msimoes@fmrp.usp.br

Leonardo Pippa Gadioli
pippagadioli@gmail.com

Luciano Fonseca Lemos de Oliveira
oliveiralfl@hotmail.com

[1] Division of Cardiology, Internal Medicine Department, Medical School of Ribeirão Preto - University of São Paulo, Ribeirão Preto, Brazil

[2] Cardiology Division – Internal Medicine Department, Hospital das Clínicas, Faculdade de Medicina de Ribeirão Preto, 3900 Bandeirantes Avenue, Ribeirão Preto, São Paulo 14048900, Brazil

cardiac systolic dysfunction is frequently preceded by left ventricular segmental wall motion impairment that predominates in the inferior, posterior-lateral, and apical regions. The finding of an isolated, thin walled, left ventricular apical aneurysm, with a "finger glove" configuration, is considered a hallmark of the disease [8].

The clinical manifestations of CCC are quite variable and may include arrhythmias with syncope or palpitations, chest pain from microvascular dysfunction, and heart failure from right and left ventricular dysfunction [9]. Cardiac conduction abnormalities are some of the first signs, especially right bundle branch block associated with left anterior fascicular block. Late manifestations include high degree atrial-ventricular block and dilated cardiomyopathy [6]. Once heart failure symptoms have presented, the prognosis is poorer than that of dilated cardiomyopathy of other etiologies [10].

Multiple imaging methods have been employed to investigate CCC patients, which were recently reviewed [11]. In particular, radionuclide imaging has been used to characterize several aspects of the cardiac involvement in CCC patients, primarily the myocardial perfusion changes and autonomic sympathetic denervation. Most recently, PET imaging has been suggested as a promising tool to detect myocardial inflammation.

Myocardial Perfusion Scintigraphy

In the clinical scenario, MPI is frequently necessary to rule out coronary artery disease (CAD) in patients with CCC because several clinical and laboratory expressions of CCC may mimic CAD, including angina pectoris and segmental LV wall motion abnormalities [12, 13]. .

Initial investigations showed that reversible myocardial perfusion defects are frequently reported in 30 to 50% of patients (Fig. 1). However, invasive coronary angiography most frequently demonstrates the absence of significant obstructive coronary disease at the epicardial vessels, indicating that the perfusion disturbance is due to coronary microvascular dysfunction [13, 14].

A pivotal study of stress-rest myocardial perfusion Thallium-201-SPECT imaging investigated 37 patients with various stages of CHD [15], independently of the presence of angina, including 12 patients without any apparent cardiac involvement; 13 patients with regional LV dysfunction, but normal global LV systolic function; and 13 patients with advanced CCC with reduced left ventricle ejection fraction (LVEF). Perfusion defects (fixed, paradoxical, and reversible) were observed in the majority (78%) of patients, and a significant topographic correlation was observed between perfusion disturbances and wall motion abnormalities that predominated in the apical and inferior-posterior-lateral LV segments. Notably, patients with more severe LV systolic dysfunction had larger myocardial perfusion defects, mainly fixed ones; a significant negative correlation between LVEF and the extent of myocardial perfusion defect (MPD) was observed. In the group of 12 patients with no other evidence of myocardial disease, 5 subjects (42%) had reversible myocardial perfusion defects, but no other kind of defects. Conspicuously, these reversible ischemic defects were mostly observed in the apical and inferior-posterior LV segments, i.e., the same regions where regional contractile dysfunction is frequently found in the later stages of CCC. These findings suggest that myocardial perfusion disturbance occurs in the early stages of CCC, preceding the start of regional LV contraction dysfunction, and may contribute to the mechanism of myocardial injury [15]. This concept was further supported by another recent investigation of 30 patients with the chronic indeterminate form using MPI; myocardial reversible perfusion defects were detected in 25% of patients and affected LV segments also exhibiting mild wall motion abnormalities [16].

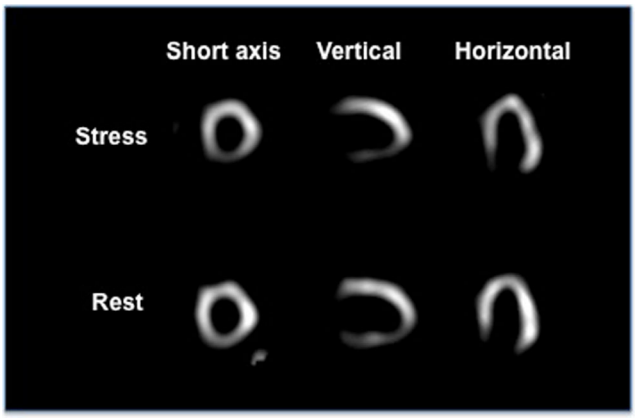

Fig. 1 Representative slices of the stress-rest SPECT imaging with Thallium-201 of a 52-year-old male patient with CCC, presenting effort angina. Moderate reversible perfusion defects are seen in the segments of the inferior wall, involving 26% of the left ventricular surface area. The angiography showed normal coronary arteries

The hypothesis that microvascular dysfunction is a component of the mechanism leading to chronic myocardial damage in CCC was further reinforced by a longitudinal, retrospective study of 36 patients with CCC [17]. Patients were initially evaluated with stress-rest MPI, and then the nuclear scans were repeated after 5.6 years. During this follow-up period, the LVEF declined significantly from 55% ± 11% to 50% ± 13%. At baseline, reversible myocardial perfusion defects were present in 20 patients (56%) and involved 10.2% of the LV area. Most notably, a topographic association was found between the presence of ischemia in the initial evaluation and the late development of wall motion abnormality in the same area; among the 47 segments with reversible perfusion defects in the initial study, 32 (68%) progressed to perfusion defects at rest (indicating the presence of fibrosis). In contrast, among the 469 segments not showing such defects in the initial study, only 41 (8.7%) had the same progression. The individual

increase in the perfusion defect area at rest was significantly correlated with the decrease of the LVEF over time. Hence, in this longitudinal study, the deterioration of LV systolic function over time was associated with both the presence of reversible ischemic defects at the initial assessment and an increase in the extent of irreversible perfusion defects, indicating regional myocardial fibrosis, during follow-up (Fig. 2) [17].

In addition to demonstrating the pathophysiological importance of microvascular ischemia for CCC progression, it has been suggested that these results indicate that SPECT MPI can achieve early detection of Chagas' disease and may be a promising tool for risk stratification and monitoring of subclinical progression of Chagas' cardiomyopathy [18].

However, the study of Hiss et al. [17] was retrospective, which limits the strength of the evidence. Of note, a prospective longitudinal study of the mechanisms that produce the myocardial damage of the late chronic phase of CCC, starting from the initial chronic indeterminate form, would require a very long follow-up period (2 to 3 decades), a significant obstacle to its execution. This obstacle justifies exploring experimental models of CCC to investigate these pathophysiological mechanisms.

Experimental Studies

Only recently, experimental studies using high-resolution imaging reported the presence of myocardial perfusion derangements in animal models of CCC, allowing characterization of the underlying histopathological myocardial tissue changes.

In the study of Lemos de Oliveira et al. [19••], myocardial perfusion defects were investigated in hamsters at the time windows of 6 and 10 months after experimental infection (chronic phase) with 3.5×10^4 to 10^5 trypomastigote forms of *T. cruzi* Y-strain. The animals were submitted to in vivo imaging, including high-resolution rest 99mTc-Sestamibi myocardial perfusion SPECT imaging and ^{18}F-FDG positron emission tomography (PET), to evaluate myocardial viability and the correlation between regional histological changes of fibrosis and inflammation. Severe myocardial perfusion defects (pixel uptake < 50% of the maximum pixel value) were present in 17 (50%) of the infected animals, involving the segments of the anterior-lateral and apical walls, ranging from 6.4 to 59% of the LV surface area. Notably, histologic analysis revealed no areas of transmural scar in those segments with rest MPD. Accordingly, those regions also had normal or only mild reduction of the ^{18}F-FDG uptake on PET images, confirming the presence of viable myocardium (Fig. 3). Infected animals with MPD had lower LV ejection fraction, higher wall motion score index on 2D-Echo, and higher inflammatory infiltrate than infected animals without MPD and controls animals.

Thus, these experimental findings show that rest MPD is associated with myocardial inflammation and does not

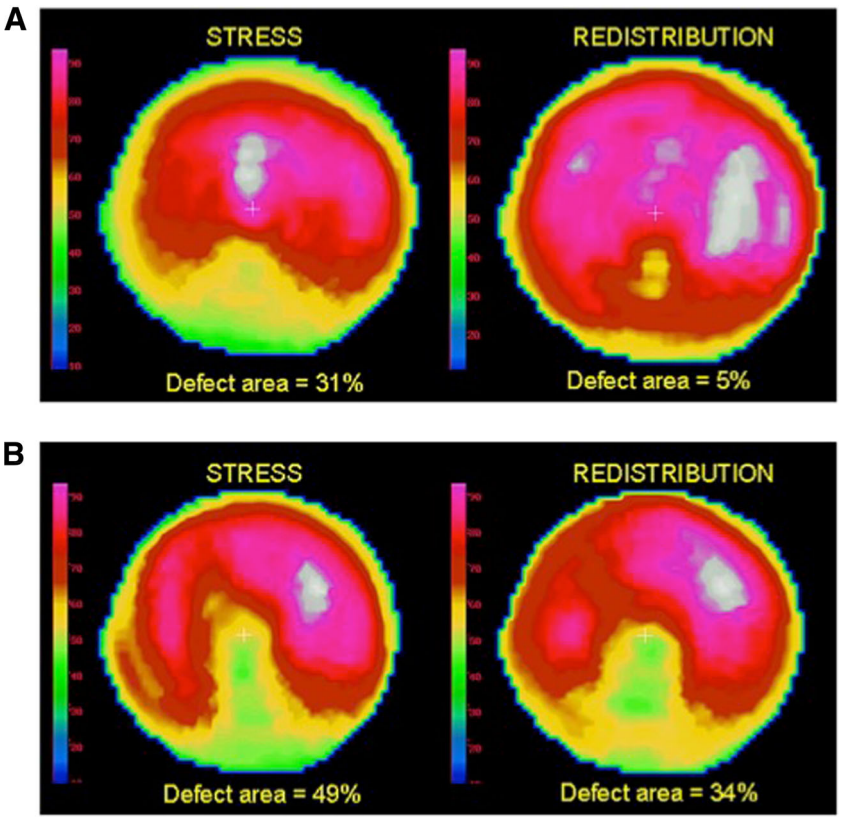

Fig. 2 Polar maps of the initial (**a**) and 6.5 year later (**b**) SPECT-Thallium-201 MPI of a patient with CCC, anginal pain, and normal coronary arteries. The interval between images was 6.5 years. A large reversible myocardial perfusion defect involving the apex, septal, inferior-septal, inferior, and inferior-lateral walls is seen in the initial study. In the late study, an extensive rest perfusion defect is observed in the same topography. Concurrently, the left ventricular ejection fraction decreases from 36 to 31% during the follow-up. (Adapted with permission from Hiss et al. [17]

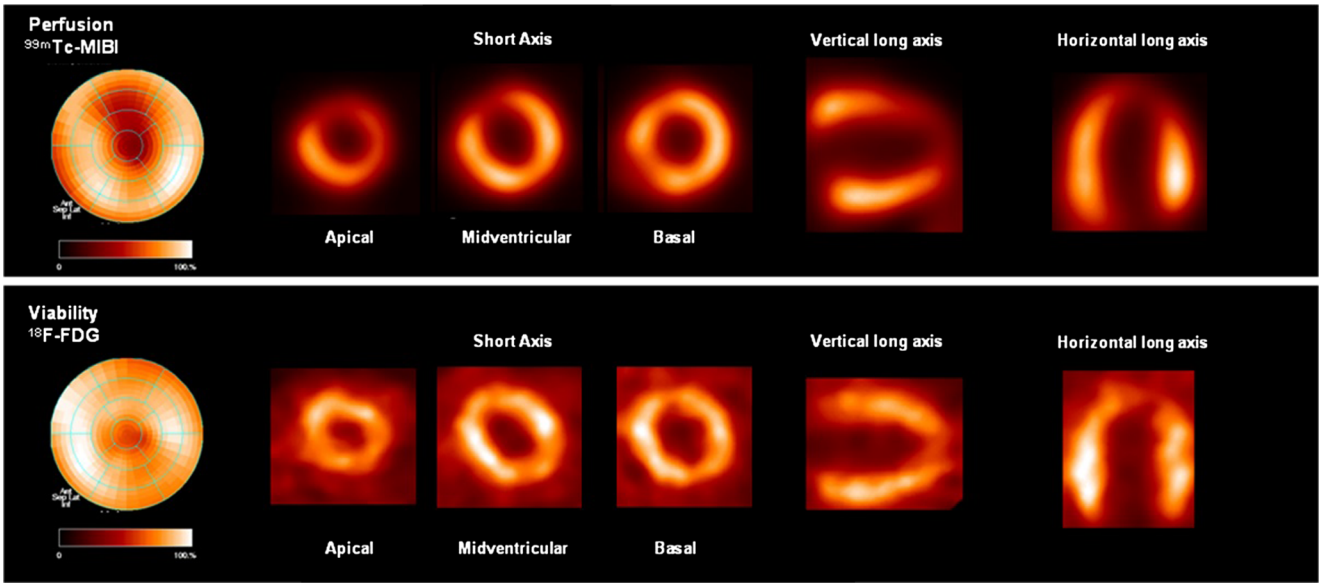

Fig. 3 High-resolution SPECT perfusion images (upper row) of a *T. cruzi*-infected animal exhibiting a severe perfusion defect (< 50% uptake) involving 29% of the LV surface area in the septum-anterior, anterior, anterior-lateral, and apical segments. Images of the corresponding ^{18}F-FDG-PET tomographic sections (lower row) show normal or mildly reduced radiotracer uptake demonstrating myocardial viability in the areas of the perfusion defect (mismatch)

indicate scar tissue, corresponding to regions with impaired wall motion but with metabolically viable myocardium.

To further investigate the hypothesis that rest myocardial perfusion defects correspond to viable hypoperfused myocardium, in the hamster experimental model of CCC, Tanaka et al. [20•] tested the effect of prolonged administration of dipyridamole, a coronary microvascular dilating drug, on the extent of rest MPD. At baseline, 6 months after experimental *T. cruzi* infection, two groups of infected animals (assigned to receive either dipyridamole or placebo) had areas of perfusion defect (13.2 ± 3.8% and 17.3 ± 3.7%, respectively) larger than the non-infected, control animal groups (assigned to receive dipyridamole or placebo; 3.8 ± 0.7% and 3.5 ± 0.9%, respectively, $p < 0.004$). After treatment, the authors observed a significant reduction of the perfusion defect area only in the infected animals treated with dipyridamole (from 17.3 ± 3.7 to 6.8 ± 2.1%, $p = 0.001$) (Fig. 4). Thus, these findings, showing amelioration of the rest myocardial perfusion following use of a microvascular-vasodilator drug, reinforce the notion that those areas correspond to viable hypoperfused myocardium [21, 22].

In summary, recent experimental in vivo imaging studies show that areas of severe rest myocardial perfusion disturbance are topographically correlated with left ventricular wall motion impairment and correspond to viable hypoperfused myocardium. This suggests the participation of microvascular ischemia in the genesis of myocardial dysfunction in CCC, a mechanism similar to the myocardial hibernation described in the ischemic cardiomyopathy of atherosclerotic origin. In addition, the findings also suggest a close relationship between myocardial perfusion derangement and inflammation, suggesting that inflammation can be the primary cause of myocardial perfusion defects in experimental CCC.

Future research, in both clinical and experimental settings, addressing the effect of therapeutic interventions with anti-inflammatory drugs and microvascular dilating agents should help to elucidate the "cause and effect" relationship between inflammation and microvascular ischemia and reveal the relative contribution of each disturbance to the pathophysiological mechanisms of CCC.

Cardiac Sympathetic Innervation Assessment Using ^{123}I-MIBG

Cardiac autonomic denervation is a conspicuous feature of CCC that was first documented by necroscopic studies describing depopulation of the parasympathetic neuronal bodies in the atrial tissue and of the sympathetic paravertebral ganglia [23, 24]. These anatomical observations were further supported by functional investigations that showed abnormal autonomic control over the sinus node function and heart rate and that demonstrated a predominant vagal denervation [25].

In recent years, myocardial scintigraphy with 123I-MIBG (MIBG) has become the main method to noninvasively assess myocardial sympathetic innervation in several forms of cardiac disease and thereby obtain accurate information about the integrity of sympathetic nerve fibers and the degree of activation of cardiac sympathetic innervation.

Our research group pioneered the use of MIBG to assess patients with CCC [15]. In a series of 37 patients with diverse degrees of LV dysfunction, regions with reduced myocardial

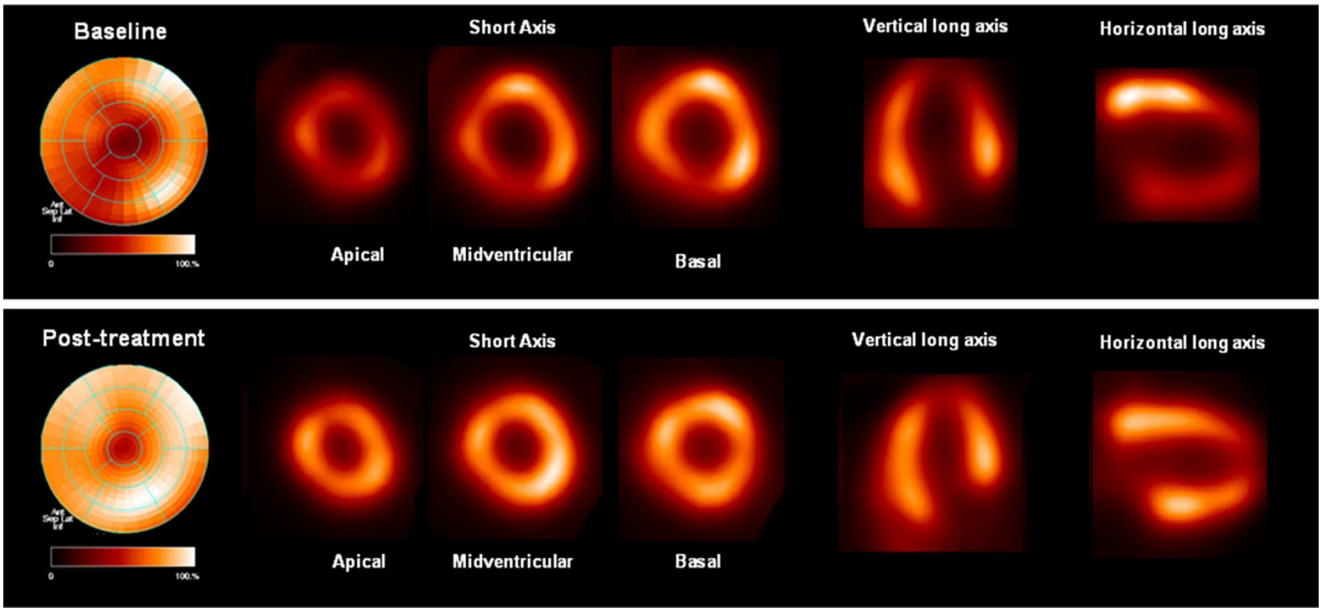

Fig. 4 Illustrative images of high-resolution rest myocardial perfusion 99m-Tc-Sestamibi-SPECT of *T. cruzi*-infected hamsters at baseline (6 months after infection) and post-treatment with dypiridamole (4 mg/kg bid, intraperitoneal, during 30 days). At baseline, there is a severe, large perfusion defect involving the septal, inferior, anterior, lateral, and apical walls. In the images acquired in the post-treatment assessment, there is a remarkable reduction of the perfusion impairment

sympathetic innervation were detected in 33% of the patients lacking another cardiac manifestation, in 77% of the patients with regional LV wall motion disturbance, and in 92% of the patients with more severe global LV systolic dysfunction. The mean areas of sympathetic denervation in each group were 3.7%, 8.3%, and 19.0% of the LV surface area, respectively. The myocardial segments exhibiting sympathetic denervation were primarily located in the apical, lateral, and inferior regions of the left ventricle.

Thus, those initial results indicated that sympathetic myocardial denervation occurs early in the course of CCC, before the establishment of the LV systolic regional or global dysfunction [15]. Moreover, there was a significant negative correlation between the area of sympathetic denervation and LVEF values, indicating that sympathetic denervation increases as myocardial dysfunction progresses, aspect well documented in other heart diseases [26]. In addition, there was a close topographic correlation among myocardial perfusion defects, LV wall motion impairment, and the areas of denervation, suggesting a pathophysiological connection between perfusion and sympathetic innervation derangements.

This possible connection was further investigated by a recent study employing image co-registration in 13 patients with CCC [27•]. It evaluated the quantitative and topographic correlation among areas of cardiac sympathetic denervation using 123I-MIBG-SPECT, myocardial hypoperfusion using Sestamibi-Tc99m-SPECT, and myocardial scarring using magnetic resonance imaging (MRI). The results showed a strong general topographic concordance between areas of denervation and areas of perfusion disturbance, suggesting that these abnormal features are correlated. The areas of stress-hypoperfused myocardium were significantly positively correlated with the areas of denervated myocardium. Moreover, the area of stress-hypoperfused myocardium corresponded to 60.8% of the denervated area, whereas only 16.1% of the denervated area corresponded to areas of fibrosis detected by MRI [27•].

Thus, those results reinforced the notion that myocardial denervation is closely correlated with myocardial hypoperfusion. In fact, repetitive hypoxia caused by microvascular ischemia may be proposed to cause injury to sympathetic nerve endings. This proposed causal pathway is supported by the observation that sympathetic nerve fibers are more sensitive to ischemic injury than cardiac muscle fibers [28, 29]. Alternatively, both types of disturbances can reflect the presence of inflammation, the underlying, damaging mechanism in CCC.

Although cardiac autonomic denervation is well characterized in patients with CCC, a clinical outcome related to this derangement was only recently reported [30]. The authors used MIBG and Tc99m-Sestamibi-SPECT imaging to prospectively investigate 15 CCC patients presenting with sustained ventricular tachycardia (SVT) and 11 patients without severe ventricular arrhythmia. The patients with SVT had higher MIBG summed defect scores (22.4 ± 9.5 vs. 10.9 ± 7.8) and more mismatch defects (correspondent to segments with viable but denervated myocardium) per patient (7.1 ± 2.0 vs. 2.0 ± 2.2) than the patients without SVT. Both groups had similar 99mTC-Sestamibi-SPECT summed defect scores (6.9 ± 7.5 vs. 4.4 ± 5.2). The detection of ≥ 3 mismatch defects was

strongly associated with the detection of SVT (93% sensitivity, 82% specificity; $p = 0.0002$). Therefore, the reported results suggested that cardiac sympathetic denervation was associated with the occurrence of severe ventricular arrhythmia in CCC (Fig. 5).

This relationship between denervation and arrhythmia was further supported by a more recent study of the quantitative correlation between the extent of sympathetic denervation and the occurrence of ventricular arrhythmia of diverse severity [31••]. In that study, 15 CCC patients with SVT had larger areas of viable but denervated myocardium, assessed by the summed difference defect scores between MIBG and Tc-99m-SPECT images (20.0 ± 8.0) than the 17 CCC patients with a less severe form of ventricular arrhythmia, i.e., non-sustained ventricular tachycardia, (11.0 ± 8.0, $p < 0.05$) and the CCC patients without a repetitive ventricular arrhythmia, based on Holter monitoring (2.0 ± 5.0, $p < 0.0001$).

Therefore, the available evidence supports the concept that cardiac sympathetic denervation may play a pivotal role in triggering severe ventricular arrhythmia in CCC. This is particularly important because severe ventricular arrhythmia in individuals with relatively preserved global left ventricular

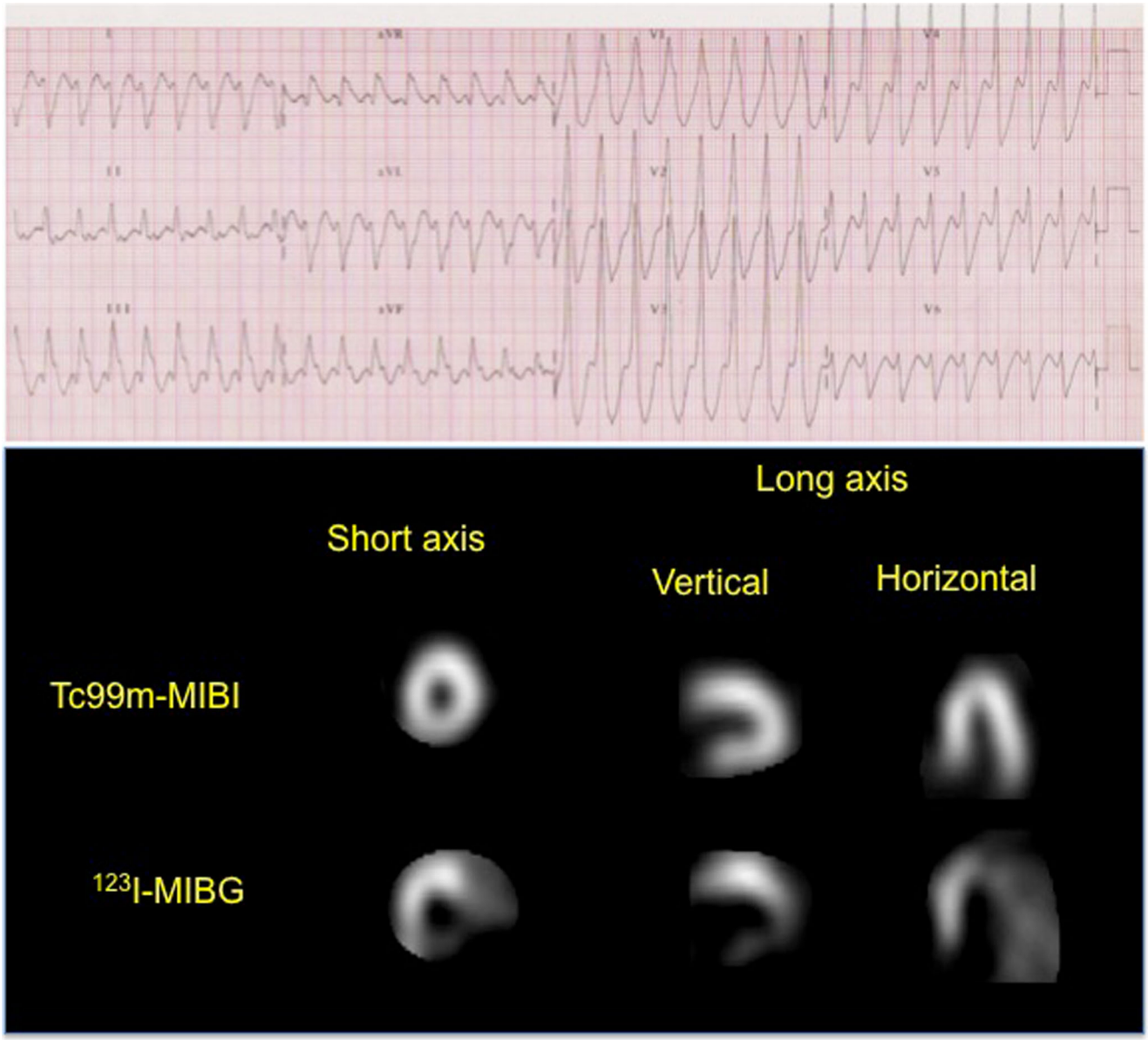

Fig. 5 ECG recordings during a sustained ventricular tachycardia induced during an invasive electrophysiological study of a patient with CCC and syncope (upper panel). The lower panel displays Tc99m-Sestamibi-SPECT and 123I-MIBG-SEPCT images of the same patient, showing severe 123-I-MIBG uptake defects in the basal and mid-ventricular portions of the inferior-lateral and inferior walls, with normal Tc99m-Sestamibi uptake, indicating the presence of viable but denervated myocardium in those regions. The ECG morphology during the induced-SVT indicates that the tachycardia originates in the same left ventricular regions where the viable denervated myocardium is located

systolic function is a typical feature of the natural history of CCC and may lead to sudden death in the early phases of disease [32]. Consequently, the available data suggest that MIBG scintigraphy can be a useful tool for risk stratification of arrhythmic sudden cardiac death in this population.

PET Imaging

Several cardiac diseases involve myocardial inflammation, which has recently become an important target of molecular imaging that may be applied to the chronic myocarditis of patients with CCC. However, the clinical use of PET imaging for evaluation of CCC patients is still limited to a few case reports.

Garg and colleagues [33] described the findings of a patient with CCC presenting with dyspnea, acute chest pain, and troponin elevation with normal coronary angiography. Echocardiography showed significant reduction of LV ejection fraction (35%) and apical and basal posterior-lateral wall aneurysms. PET imaging with ammonia (13NH3) revealed myocardial perfusion defects at the apex, basal inferior-lateral, and lateral walls. The 18F-FDG PET images, using an appropriate protocol for suppression of glucose uptake by cardiomyocytes, displayed high uptake of the radiotracer partially overlapping the regions exhibiting perfusion defects, suggesting myocardial inflammation, especially, in regions adjacent to perfusion defects and LV aneurysms. Another case with very similar characteristics was recently reported [34].

Recently, Shapiro and colleagues [35] reported two patients with CCC with clinical presentation of arrhythmic storm with recurrent ventricular tachycardia (VT). They demonstrated that a higher uptake of 18F-FDG was partially correlated with the myocardial regions where the VT originated, supporting the contribution of on-going inflammation to the mechanism of VT. This observation is particularly important due to the higher risk of cardiac events in CCC patients presenting with VT.

Taken together, these results suggest that active inflammation may contribute to myocardial perfusion disturbances and conduction abnormalities leading to myocardial dysfunction and severe ventricular arrhythmia potentially associated with sudden cardiac death. Thus, in vivo detection of inflammation with 18F-FDG-PET is a promising tool to monitor disease activity and risk stratification of patients with CCC. Future research should address these new potential clinical applications of PET imaging.

Conclusions

Findings from clinical studies and recent experimental investigations using high-resolution SPECT MPI emphasized the involvement of microvascular ischemia in the progression of CCC. Furthermore, MPI can detect evidence of subclinical myocardial damage early and so is a promising non-invasive tool for monitoring the disease progression.

Cardiac autonomic denervation, assessed by 123I-MIBG, can be detected even in patients with no other manifestations of heart disease. Notably, the extent of sympathetic denervation correlates with the occurrence and severity of ventricular arrhythmia, indicating that this image technique can be used to stratify the risk of sudden death in CCC patients.

Future research in CCC should address the effectiveness of MPI and PET for monitoring early subclinical myocardial damage to evaluate therapeutic strategies targeting inflammation and microvascular ischemia.

Compliance with Ethical Standards

Conflict of Interest Marcus Vinicius Simões, Leonardo Pippa Gadioli, and Luciano Fonseca Lemos de Oliveira declare that they have no conflict of interest.

Human and Animal Rights and Informed Consent This article does not contain any studies with human or animal subjects performed by any of the authors.

Publisher's Note Springer Nature remains neutral with regard to jurisdictional claims in published maps and institutional affiliations.

References

Papers of particular interest, published recently, have been highlighted as:
- • Of importance
- •• Of major importance

1. Chagas disease in Latin America: an epidemiological update based on 2010 estimates. World Health Organization. Wkly Epidemiol Rec. 2015;90:33–43.
2. Benziger CP, do Carmo GA, Ribeiro AL. Chagas cardiomyopathy: clinical presentation and management in the Americas. Cardiol Clin. 2017;35:31–47.
3. Requena-Méndez A, Aldasoro E, de Lazzari E, Sicuri E, Brown M, Moore DAJ, et al. Prevalence of Chagas disease in Latin-American migrants living in Europe: a systematic review and meta-analysis. PLoS Negl Trop Dis. 2015;9:e0003540.
4. Traina MI, Hernandez S, Sanchez DR, Dufani J, Salih M, Abuhamidah AM, et al. Prevalence of Chagas disease in a U.S. population of Latin American immigrants with conduction abnormalities on electrocardiogram. PLoS Negl Trop Dis. 2017;11:e0005244.
5. Dias JC. The indeterminate form of human chronic Chagas' disease. A clinical epidemiological review. Rev Soc Bras Med Trop. 1989;22:147–56.
6. Bocchi EA, Bestetti RB, Scanavacca MI, Cunha Neto E, Issa VS. Chronic Chagas heart disease management: from etiology to cardiomyopathy treatment. J Am Coll Cardiol. 2017;70:1510–24.
7. Marin-Neto JA, Cunha-Neto E, Maciel BC, Simões MV. Pathogenesis of chronic Chagas heart disease. Circulation. 2007;115:1109–23.

8. Simões MV, Oliveira LF, Hiss FC, Figueiredo AB, Pintya AO, Maciel BC, et al. Characterization of the apical aneurysm of chronic Chagas' heart disease by scintigraphic image co-registration. Arq Bras Cardiol. 2007;89(2):119–21 **131-4**.
9. Velasco A, Morillo CA. Chagas heart disease: a contemporary review. J Nucl Cardiol. 2018. https://doi.org/10.1007/s12350-018-1361-1.
10. Ayub-Ferreira SM, Mangini S, Issa VS, Cruz FD, Bacal F, Guimarães GV, et al. Mode of death on Chagas heart disease: comparison with other etiologies. A subanalysis of the REMADHE prospective trial. PLoS Negl Trop Dis. 2013;7(4):e2176.
11. Nunes MCP, Badano LP, Marin-Neto JA, Edvardsen T, Fernández-Golfín C, Bucciarelli-Ducci C, et al. Multimodality imaging evaluation of Chagas disease: an expert consensus of Brazilian cardiovascular imaging department (DIC) and the European Association of Cardiovascular Imaging (EACVI). Eur Heart J Cardiovasc Imaging. 2018;19(4):459–460n. https://doi.org/10.1093/ehjci/jex154.
12. Feit A, El-Sherif N, Korostoff S. Chagas' disease masquerading as coronary artery disease. Arch Intern Med. 1983;143(1):144–5.
13. Hagar JM, Rahimtoola SH. Chagas' heart disease in the United States. N Engl J Med. 1991;325(11):763–8.
14. Marin-Neto JA, Marzullo P, Marcassa C, Gallo Junior L, Maciel BC, Bellina CR, et al. Myocardial perfusion abnormalities in chronic Chagas' disease as detected by thallium-201 scintigraphy. Am J Cardiol. 1992;69(8):780–4.
15. Simoes MV, Pintya AO, Bromberg-Marin G, Sarabanda AV, Antloga CM, Pazin-Filho A, et al. Relation of regional sympathetic denervation and myocardial perfusion disturbance to wall motion impairment in Chagas' cardiomyopathy. Am J Cardiol. 2000;86(9):975–81.
16. Peix A, Garcia R, Sanchez J, Cabrera LO, Padron K, Vedia O, et al. Myocardial perfusion imaging and cardiac involvement in the indeterminate phase of Chagas disease. Arq Bras Cardiol. 2013;100(2):114–7.
17. Hiss FC, Lascala TF, Maciel BC, Marin-Neto JA, Simoes MV. Changes in myocardial perfusion correlate with deterioration of left ventricular systolic function in chronic Chagas' cardiomyopathy. J Am Coll Cardiol Img. 2009;2(2):164–72.
18. Schwartz RG, Wexler O. Early identification and monitoring progression of Chagas' cardiomyopathy with SPECT myocardial perfusion imaging. JACC Cardiovasc Imaging. 2009;2(2):173–5.
19.•• Lemos de Oliveira LF, Thackeray JT, Marin Neto JA, Dias Romano MM, Vieira de Carvalho EE, Mejia J, et al. Regional Myocardial Perfusion Disturbance in Experimental Chronic Chagas Cardiomyopathy. J Nucl Med. 2018;59(9):1430–6 **This paper is the first to describe the findings of high-resolution SPECT perfusion and ^{18}F-FDG PET images in a experimental model of chronic chagas disease in hamsters, showing the correlation between myocardial perfusion disturbance and underlying inflammatory changes.**
20.• Tanaka DM, de Oliveira LFL, Marin-Neto JA, Romano MMD, de Carvalho EEV, de Barros Filho ACL, et al. Prolonged dipyridamole administration reduces myocardial perfusion defects in experimental chronic Chagas cardiomyopathy. J Nucl Cardiol. 2018. https://doi.org/10.1007/s12350-018-1198-7 **In this paper, the authors show the improvement of myocardial perfusion following the chronic administration of a microvascular dilator agent, reinforcing the hypothesis of participation of myocardial ischemia in the mechanism leading to cardiac dysfunction progression in CCC.**
21. Marin-Neto JA, Simões MV, Rassi Junior A. Pathogenesis of chronic Chagas cardiomyopathy: the role of coronary microvascular derangements. Rev Soc Bras Med Trop. 2013;46(5):536–41.
22. Petretta M, Cuocolo A. The long way to defeating Chagas cardiomyopathy. J Nucl Cardiol. 2018. https://doi.org/10.1007/s12350-018-1238-3.
23. Köberle F. Cardiopathia parasympaticopriva. München Med Wschr. 1959;101:1308–10.
24. Mott KE, Hagstrom JW. The pathologic lesions of the cardiac autonomic nervous system in chronic Chagas' myocarditis. Circulation. 1965;31:273–86.
25. Marin-Neto JA, Bromberg-Marin G, Pazin-Filho A, Simões MV, Maciel BC. Cardiac autonomic impairment and early myocardial damage involving the right ventricle are independent phenomena in Chagas' disease. Int J Cardiol. 1998;65:261–9.
26. Marino VSP, Dumont SM, Mota LDG, Braga DS, Freitas SS, Moreira MDCV. Sympathetic Dysautonomia in heart failure by 123I-MIBG: comparison between Chagasic, non-Chagasic and heart transplant patients. Arq Bras Cardiol. 2018 Aug;111(2):182–90.
27.• Barizon GC, Simões MV, Schmidt A, Gadioli LP, Murta-Junior LO. Relationship between microvascular changes, autonomic denervation, and myocardial fibrosis in Chagas cardiomyopathy: evaluation by MRI and SPECT imaging. J Nucl Cardiol. 2018. https://doi.org/10.1007/s12350-018-1290-z **This papers describes, by employing multiple imaging modalities corregistration in patients with CCC, the close topographic and quantitative correlation among microvascular ischemia and sympathetic denervation.**
28. Bengel FM, Barthel P, Matsunari I, Schmidt G, Schwaiger M. Kinetics of 123I-MIBG after acute myocardial infarction and reperfusion therapy. J Nucl Med. 1999 Jun;40(6):904–10.
29. Simões MV, Barthel P, Matsunari I, Nekolla SG, Schömig A, Schwaiger M, et al. Presence of sympathetically denervated but viable myocardium and its electrophysiologic correlates after early revascularised, acute myocardial infarction. Eur Heart J. 2004 Apr;25(7):551–7.
30. Miranda CH, Figueiredo AB, Maciel BC, Marin-Neto JA, Simoes MV. Sustained ventricular tachycardia is associated with regional myocardial sympathetic denervation assessed with 123I-metaiodobenzylguanidine in chronic Chagas cardiomyopathy. J Nucl Med. 2011;52(4):504–10.
31.•• Gadioli LP, Miranda CH, Pintya AO, de Figueiredo AB, Schmidt A, Maciel BC, et al. The severity of ventricular arrhythmia correlates with the extent of myocardial sympathetic denervation, but not with myocardial fibrosis extent in chronic Chagas cardiomyopathy: Chagas disease, denervation and arrhythmia. J Nucl Cardiol. 2018;25(1):75–83 **This paper shows a quantitative correlation between the extent of sympathetic denervation and the severity of incident ventricular arrhythmia, indicating a potential role of MIBG imaging in risk stratify the risk of sudden death in CCC patients.**
32. Rassi A Jr, Rassi SG, Rassi A. Sudden death in Chagas' disease. Arq Bras Cardiol. 2001;76(1):75–96.
33. Garg G, Cohen S, Neches R, Travin MI. Cardiac (18)F-FDG uptake in chagas disease. J Nucl Cardiol. 2016;23(2):321–5.
34. Salimy MS, Parwani PJ, Mukai K, Pampaloni MH, Flavell RR. Abnormal ^{18}F-FDG and ^{82}Rb PET findings in Chagas heart disease. Clin Nucl Med. 2017;42(5):e265–8.
35. Shapiro H, Meymandi S, Shivkumar K, Bradfield JS. Cardiac inflammation and ventricular tachycardia in Chagas disease. Heart Rhythm Case Rep. 2017;3(8):392–5. https://doi.org/10.1016/j.hrcr.2017.05.007 eCollection 2017 Aug.